

Article

Determination of Pore and Surface Diffusivities from Single Decay Curve in CSBR Based on Parallel Diffusion Model

Yoshimi Seida ^{1,*} , Noriyoshi Sonetaka ², Kenneth E. Noll ³ and Eiji Furuya ^{4,*}¹ Natural Science Laboratory, Toyo University, Bunkyo-ku, Tokyo 112-8606, Japan² TechnoMediaLab, Inc., Minato-ku, Tokyo 108-0075, Japan³ Department of Civil, Architectural and Environmental Engineering, Illinois Institute of Technology, Chicago, IL 60616, USA⁴ Department of Applied Chemistry, Meiji University, Kawasaki 214-8571, Japan

* Correspondence: seida@toyo.jp (Y.S.); egfuruya@meiji.ac.jp (E.F.); Tel.: +81-3-3945-4894 (Y.S.)

Abstract: A novel, simple numerical method to determine the pore and surface diffusivities in adsorbents from a single experimental concentration decay curve obtained using the batch adsorption technique was investigated in this study. The pore and surface diffusion coefficients were determined based on the conventional parallel diffusion model in its dimensionless form using a theoretical model correlation. The model assumed that the film mass transfer resistance was negligible, i.e., the condition with a large Biot number, from the single concentration decay curve. The procedure for determining the kinetic parameters was investigated, and the effectiveness of the proposed simple method was validated by comparing the parameters with those reported previously. The single decay curve of *p*-nitrophenol, obtained by the batch adsorption system using granular activated carbon as an adsorbent, was used for validation. The diffusivities determined by the simple method corresponded fairly well with the diffusivities reported previously.



Citation: Seida, Y.; Sonetaka, N.; Noll, K.E.; Furuya, E. Determination of Pore and Surface Diffusivities from Single Decay Curve in CSBR Based on Parallel Diffusion Model. *Water* **2022**, *14*, 3629. <https://doi.org/10.3390/w14223629>

Academic Editors: Silvia Santos, Ariana Pintor and Antonio Turco

Received: 9 October 2022

Accepted: 7 November 2022

Published: 11 November 2022

Publisher's Note: MDPI stays neutral with regard to jurisdictional claims in published maps and institutional affiliations.



Copyright: © 2022 by the authors. Licensee MDPI, Basel, Switzerland. This article is an open access article distributed under the terms and conditions of the Creative Commons Attribution (CC BY) license (<https://creativecommons.org/licenses/by/4.0/>).

Keywords: adsorption; diffusion; parallel diffusion model; completely mixed batch reactor

1. Introduction

Equilibrium and kinetic properties are essential for the design of adsorptive separation and purification apparatus. In liquid-phase adsorption systems, the adsorption isotherms are usually determined using the batch bottle technique. The Freundlich- or Langmuir-type equations are frequently used to correlate equilibrium adsorption data that have been obtained experimentally. Kinetic parameters such as the film resistance coefficient and diffusion coefficient of adsorbents are obtained from the adsorption data, such as breakthrough curves (BTC) in fixed-bed adsorbers, adsorption uptake curves in the shallow-bed technique, and concentration decay curves in a completely mixed batch reactor (CMBR) [1]. During the design of adsorptive separation reactors, a methodological study to determine the kinetic parameters is essential. The adsorption model is generally estimated by fitting the model prediction with the experimentally obtained adsorption data, along with the determination of the kinetic parameters. For example, when a Bangham plot of experimentally collected adsorption data shows a linear correlation that obeys the Bangham equation, the adsorption process is pore diffusion control. If not, fitting of the adsorption data by other adsorption models, such as the surface diffusion model, homogeneous intraparticle diffusion model, and multiple diffusion models, will be performed one-by-one to determine the adsorption mechanism and the kinetic parameters. Many studies determining the adsorption model through the procedure mentioned above have been reported [2–7]. From an economic and temporal point of view, it would be desirable to determine the reliable kinetic parameters using a simple method with a small number of experiments. The engineering needs for simple, rapid, and cost-effective determination methods are always high because of the complexity of determining multiple kinetic parameters and

cost issues, especially in systems with multiple transfer modes. When the fixed-bed adsorption technique is used for the determination of the kinetic parameters, axial diffusion, channeling, and particle boundary film diffusion may occur. To eliminate these effects, a shallow-bed method can be used. However, its demerit is the use of a large amount of test fluid for each run (approximately 200 L, for instance), which causes environmental pollution when discharged. In contrast, the advantage of the CMBR method is its simplicity of data acquisition, with a smaller amount of test fluid for each run. Automation of the experimental equipment and data acquisition is possible. However, the disadvantage of using the CMBR method is predicting the reliable mass transfer resistance within the film accurately. Mass transfer in the adsorption phase of the adsorbents is taken into consideration for the mass transfer of adsorbates from fluid to granular activated carbon particles. This is because surface diffusion, which occurs in the transfer on the solid phase of the adsorbents, becomes dominant in the adsorption process of the adsorbents with an increase in adsorption amount and mass transfer in the pore phase [8]. Several experimental results must be analyzed separately based on quasi-linear equilibrium assumptions to determine the pore and surface diffusivities in this type of adsorbent with binary mode mass transfer.

The surface diffusion of adsorbents has been observed in many adsorbent systems [9–12]. Medved et al. reviewed the surface diffusion models of various adsorbents [13]. In a continuous flow column separation system following an ideal single adsorption diffusion model, the BTC of the system shows a symmetrical S-shaped sigmoidal curve. The tailing of BTCs is often observed in adsorbents with large adsorption capacities and multiple diffusion mechanisms. However, the conventional pore diffusion model, the primary single adsorption diffusion model, is unable to predict BTCs with tailing [14]. Hence, a parallel diffusion model is a representative candidate for the successful prediction of BTCs in this case. The parallel diffusion model deals with intraparticle pore diffusion and surface diffusion processes in adsorbents. The tailing of the BTCs in the packed-bed reactors and the decay curves in the CMBR system can be predicted using the model. Although the determination of the multiple kinetic parameters in the model is time-consuming and requires much adsorption data in practice, the tailing of the adsorption curves can be predicted well using the model with binary mode transfer mechanisms.

Several methods have been developed to determine the kinetic parameters of adsorption models using multiple transfer modes. One of the methods is the independent determination of the kinetic parameters using correlation equations available in the literature and theoretical models, independent of the adsorption experiment. Another method is the model-fitting approach, in which the kinetic parameters are determined by fitting the decay curves or BTCs calculated using diffusion models to the experimentally obtained curves. The former approach is useful for confirming the trends of the adsorption data simply and rapidly. However, the calculated kinetic parameters deviate significantly from the experimental adsorption data; thus, further adjustment of the kinetic parameters is required. The latter method requires cumbersome numerical calculations and trial-and-error data fitting to determine the kinetic parameters. It is also necessary to collect multiple experimental data under various conditions, such as the initial adsorbate concentration and agitation/flow rates, to determine multiple parameters [15–17].

Souza et al. [18,19] and Valderrama et al. [20] reported a method for determining the kinetic parameters in a parallel diffusion model in a continuous stirred tank reactor (CSTR). First, the boundary film resistance coefficient (k_f) was determined from the initial slope of the decay curves in the CSTR, since the intraparticle diffusion influence is minimal at this stage. The pore diffusion coefficient (D_p) was independently calculated from the molecular diffusion coefficient obtained from Wilke and Chang's equation [21] and the tortuosity factor of the adsorbent. Subsequently, they determined the surface diffusion coefficient (D_s) by curve fitting of the decay curve simulated using the determined k_f and D_p values.

Liu et al. studied a parallel diffusion model for a column separation system of levulinic acid [22,23]. They determined the k_f using the Wilson–Geankoplis correlation equation. The D_s and D_p were determined from batch adsorption experiments. The concentration

decay curves obtained by the batch adsorption experiments were fitted and compared with the model predictions using the single pore diffusion, single surface diffusion, and parallel diffusion models. The influence of the diffusion coefficient towards the concentration decay curves in the models was observed. The parallel diffusion model simulated the column separation of levulinic acid efficiently using the kinetic parameters determined from batch adsorption experiments.

Yao et al. studied a simple method to determine the k_f and D_s without calculating the diffusion equations in a batch adsorption system [24]. The k_f was determined by fitting the early-stage concentration decay curve obtained from a batch adsorption experiment with an early-stage kinetic equation. The D_s was then determined by fitting the late-stage decay curve with an approximate equation for the analytical solution of the diffusion equation. The obtained kinetic parameters were applied to other adsorption systems to validate the accuracy of the method.

Chung et al. examined a method for determining the kinetic parameters in a parallel diffusion model in a column adsorption system using frontal analysis [25]. The D_p was first determined using frontal analysis. BTC prediction was performed using the parallel diffusion model with D_p obtained from frontal analysis. The D_s was calculated using the best fitting obtained from the model predictions to the experimental BTC data.

Danica et al. applied the high-order frequency response function obtained by nonlinear frequency response analysis to pore diffusion analysis [26]. They successfully applied the pioneering research of the frequency response analysis performed by Petkovska et al. [27] to separately estimate the pore and surface diffusion coefficients.

When a shallow bed or CMBR is used, experimental conditions with negligible film mass transfer resistance are available, as mentioned above. It is easy to obtain the pore diffusion and surface diffusion coefficients simultaneously from the concentration decay curves under film-resistance-free conditions. In this study, we focused on the parallel diffusion model and a simple determination method for the multiple kinetic parameters of the model using the CMBR method. The simple method to determine the pore and surface diffusivities of adsorbents under negligible film resistance conditions was investigated based on a theoretical model analysis of a non-dimensional parallel diffusion model using a theoretical model correlation. The time ratio of the concentration decay curves ($T_{0.2}/T_{0.8} = T(C/C_0 = 0.2)/T(C/C_0 = 0.8)$) and the diffusivity ratio between pore and surface diffusion (R_D) were successfully correlated based on the parallel diffusion model. The time ratio characterizes the decay curve as a single parameter. This correlation was used to determine the diffusivities from the single concentration decay curve. The effectiveness of the method was confirmed using the adsorption data of a *p*-nitrophenol/activated carbon system obtained by the CMBR method. The adsorbate/adsorbent system is known to be surface-diffusion-dominant, with large Freundlich n values [28,29].

2. Parallel Diffusion Model in Dimensionless Form

This study assumes the diffusive adsorption of organic adsorbates in highly affinitive spherical porous adsorbents. The adsorption model assumes that mass transfer in the adsorbent is the rate-limiting step of the adsorption rate. Adsorbents with Freundlich-type adsorption isotherms were considered in this study because the Freundlich type is often observed in adsorbents with surface diffusion transfer. However, the simple method developed in this study is applicable to different types of adsorption isotherms. In a liquid-phase adsorption separation system, the mass transfer process in the film at the fluid-to-solid interface and inside the adsorbents controls the adsorption rate, rather than the adsorption equilibrium at the adsorption sites in the adsorbents. The intraparticle transport of adsorbates via pore and surface diffusion in the adsorbents is considered in the ordinary parallel diffusion model. In a system with surface diffusion, the adsorbates are distributed in the adsorption phase rather than in the pore phase. This assumption corresponds to the Freundlich-type adsorption isotherm, $q = kc^{1/n}$, with high k and n values. Assuming that the porosity and packed density of the adsorbents are ε and ρ_s , respectively,

the amount of adsorbate in the pores and the solid in a certain volume of the adsorbent V are denoted by ϵVc and $V\rho_s kc^{1/n}$, respectively. The ratio of the amounts of adsorbates in the solid to the pores is expressed by $\rho_s kc^{1/n-1}/\epsilon$. Figure 1 shows the ratio as a function of n and c . The value of $\rho_s k/\epsilon$ is not small but more than ten in general; thus, the ratio is very large in the adsorbents with n values greater than unity, indicating the small contribution of pore diffusion transfer.

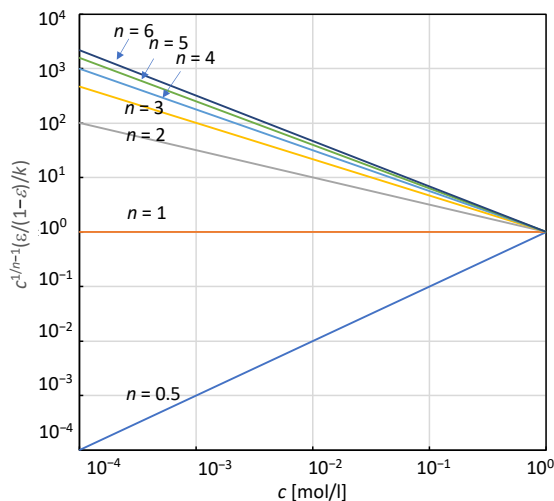


Figure 1. Distribution ratio of adsorbate.

For the CMBR method, the fundamental single-mode mass transfer system equations in the dimensional form are as follows.

Intraparticle diffusion: here, q_m and D_s are the amount of adsorption at radius r in the adsorbent and the surface diffusion coefficient, respectively.

$$\left(\frac{\partial q_m}{\partial t}\right) = \left(\frac{D_s}{r^2}\right) \frac{\partial}{\partial r} \left(r^2 \frac{\partial q_m}{\partial r}\right) \tag{1}$$

Fluid-to-solid film transport:

$$\rho_s \left(\frac{\partial q_t}{\partial t}\right) = k_f a_p (c_t - c_s) \tag{2}$$

where k_f , a_p , c_t and c_s are the film mass transfer coefficient, surface area, concentration in the vessel and fluid concentration at $r = r_p$, respectively.

Interface transport:

$$\left(\frac{\partial q_t}{\partial t}\right) = -a_p D_s \left(\frac{\partial q_m}{\partial r}\right)_{r=r_p} \tag{3}$$

Mass balance within vessel:

$$\left(\frac{\partial q_t}{\partial t}\right) = -\left(\frac{V}{m}\right) \left(\frac{\partial c_t}{\partial t}\right) \tag{4}$$

at $t = 0$, $q_t = 0$ and $c_t = c_0$.

Average amount adsorbed:

$$q_t = \frac{\int_0^{r_p} 4\pi q_m r^2 dr}{\left(\frac{4}{3}\right) \pi r_p^3} \tag{5}$$

q_t is the amount of adsorbate in the adsorbent.

Adsorption equilibrium:

$$q_s = kc_t^{\frac{1}{n}} \tag{6}$$

In the case of the parallel diffusion model, which is free from film diffusion resistance, the fundamental equations are as follows.

Intraparticle diffusion:

$$\rho_s \left(\frac{\partial q_m}{\partial t} \right) = \rho_s \left(\frac{D_s}{r^2} \right) \frac{\partial}{\partial r} \left(r^2 \frac{\partial q_m}{\partial r} \right) + \left(\frac{D_p}{r^2} \right) \frac{\partial}{\partial r} \left(r^2 \frac{\partial c_m}{\partial r} \right) \tag{7}$$

with initial and boundary conditions $q_m = 0$ at $t = 0$ and $q_m = f(c_t)$ at $r = r_p$.

The accumulation term on the left-hand side of Equation (7) considers only the adsorption phase because of the small distribution of adsorbates in the pores. The first and second terms on the right-hand side of the equation are the fluxes due to surface diffusion and pore diffusion, respectively. The average amount adsorbed and the equilibrium relationship are the same as in Equations (5) and (6).

As the equations contain many constants and variables, they were converted to dimensionless variables using dimensionless variables, as shown below.

Dimensionless variables:

$$T = \left(\frac{D_s}{r_p^2} \right) t, \quad R = \left(\frac{R}{r_p} \right), \quad C_t = \left(\frac{c_t}{c_0} \right), \quad C_s = \left(\frac{c_s}{c_0} \right), \quad Q_t = \left(\frac{q_t}{q_0} \right), \quad Q_m = \left(\frac{q_m}{q_0} \right)$$

For the CMBR method, the dimensionless equations are shown as follows.

Intraparticle diffusion:

$$\left(\frac{\partial Q_m}{\partial T} \right) = \left(\frac{1}{R^2} \right) \frac{\partial}{\partial R} \left(R^2 \frac{\partial Q_m}{\partial R} \right) \tag{8}$$

$$- \left(\frac{\partial Q_m}{\partial R} \right)_{R=1} = B_i (C_t - C_s) \tag{9}$$

where $B_i = \frac{k_f r_p}{D_s \beta \rho_s}$

$$\left(\frac{\partial Q}{\partial T} \right) = \frac{1}{R^2} \frac{\partial}{\partial R} \left(R^2 \frac{\partial Q_m}{\partial R} \right) + R_D \left(\frac{1}{R^2} \right) \frac{\partial}{\partial R} \left(R^2 \frac{\partial C_m}{\partial R} \right) \tag{10}$$

where $R_D = \frac{D_p}{D_s \beta \rho_s}$, and the initial and boundary conditions are $Q_m = 0$ at $T = 0$.

R_D denotes the ratio of diffusion resistance owing to surface diffusion and pore diffusion, and $V/m\beta$ is the dimensionless fluid-to-solid ratio.

Mass balance within the vessel:

$$\left(\frac{\partial Q_t}{\partial T} \right) = - \left(\frac{V}{m\beta} \right) \left(\frac{\partial C_t}{\partial T} \right) \tag{11}$$

Average amount adsorbed:

$$Q_t = 3 \int_0^1 Q_m R^2 dR \tag{12}$$

Equilibrium relationship:

$$Q_s = C_t^{\frac{1}{n}} \tag{13}$$

The series of equations in non-dimensional form was solved numerically using the finite difference method. The details of the numerical calculations are reported by Fujiki et al. [30].

3. Results and Discussion

3.1. R_D Dependence of Adsorption Profiles and Decay Curves

The model simulation of the parallel diffusion model has been reported in the literature, but no study has been reported on the mass distribution in the adsorbents in relation to the contribution of the diffusion mode, despite the importance of using separation properties to understand the adsorbents. The distributions in the spherical adsorbent are shown in Figure 2a–d for some specific cases with different diffusion modes. The intraparticle distributions of the adsorbate in the pore (C_m) and the solid (Q_m) differ significantly depending on the R_D value. As seen in these figures, the adsorption profiles changed significantly from a gentle to a sharp distribution with a steep adsorption front depending on the R_D value. This is attributed to the difference in transfer resistance between the pores and the adsorbent surface. In the large R_D system, adsorption profiles with a steep adsorption front appear because of the large surface diffusion resistance, as shown in Figure 2b,d. In contrast, the small R_D system results in an adsorption profile penetrating deep inside the adsorbent because of the faster surface diffusion.

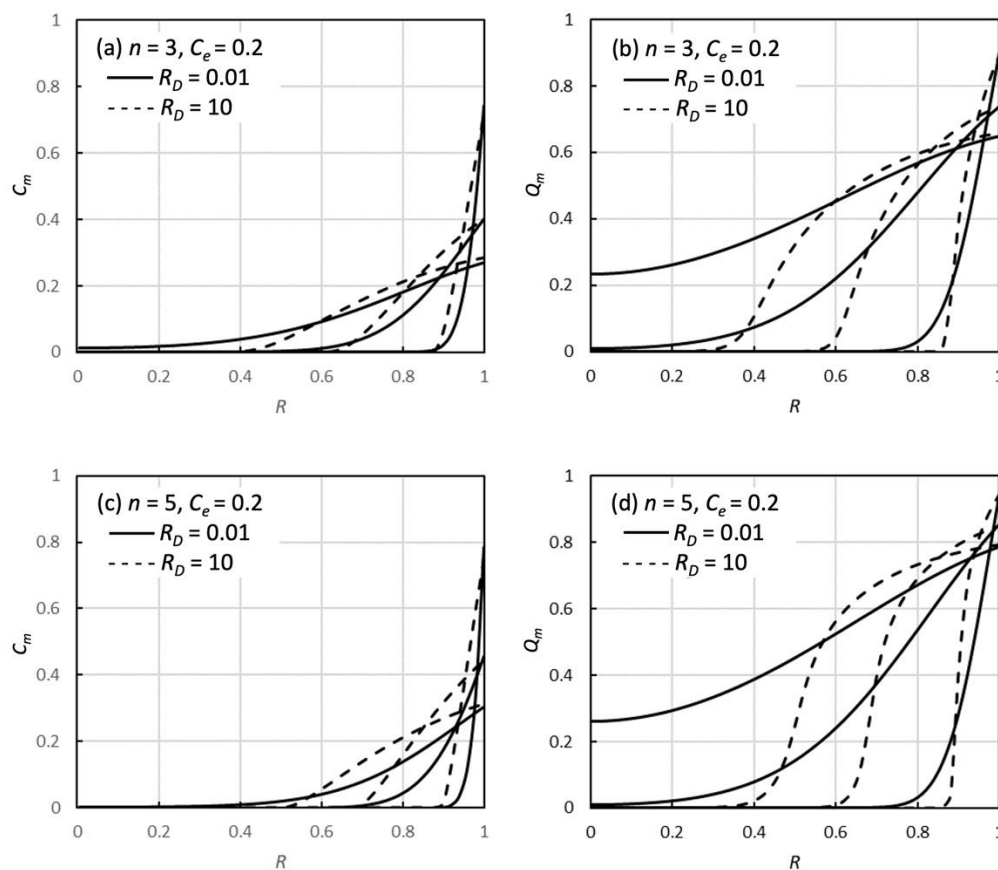


Figure 2. Distribution of adsorbate in the adsorbent particles. (a) C_m , $n = 3$, (b) Q_m , $n = 3$, (c) C_m , $n = 5$, (d) Q_m , $n = 5$. The bold lines indicate the distribution in the case of $R_D = 0.01$ at $T = 4 \times 10^{-3}$, 4×10^{-2} and 1×10^{-1} , respectively. The dotted lines indicate the distribution in the case of $R_D = 10$ at $T = 4 \times 10^{-4}$, 4×10^{-3} and 1×10^{-2} .

Figure 3 shows some examples of the concentration decay curves in the CMBR in the cases of $R_D = 0.01$ ($n = 3, 5$) and 10 ($n = 3, 5$). Faster transport through pore diffusion in the case of a large R_D results in a rapid concentration decay. A smaller R_D system results in a slow concentration decay with long tailing. The total adsorbate flux in the adsorbent decreases with an increase in the n value due to the increase in adsorption and slow surface diffusion, and thus the decay becomes slow with the increase in the n value.

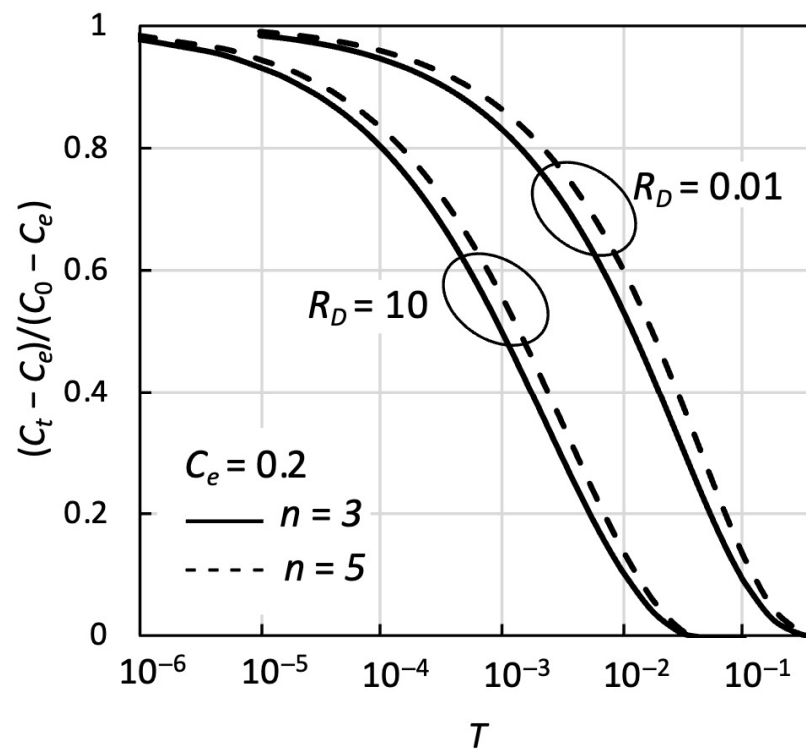


Figure 3. The concentration decay curves simulated by the model under study.

3.2. Determination of the Time Ratio $T_{0.2}/T_{0.8}$ from Concentration Decay Curves

The pore and surface diffusivities in the parallel diffusion model were determined from a single concentration decay curve using the following procedure, in principle, with the simultaneous determination of the intraparticle diffusivity and fluid-to-solid mass transfer coefficient. First, dimensionless concentration decay curves were obtained from the model simulation. The concentration decay curve C_t vs. T graph was plotted, as shown in Figure 4a. Then, the vertical axis of the concentration decay curve was transformed into a new normalized variable, $(C_t - C_e)/(C_0 - C_e)$. Irrespective of the experimental conditions, the values of the numerical concentration decay curve (NCDC) can be expressed between zero and unity by transforming the data (Figure 4b). The values of $T_{0.8}$ and $T_{0.2}$ are defined by reading the decay curve at $(C_t - C_e)/(C_0 - C_e) = 0.8$ and 0.2 , respectively, as shown in Figure 4b.

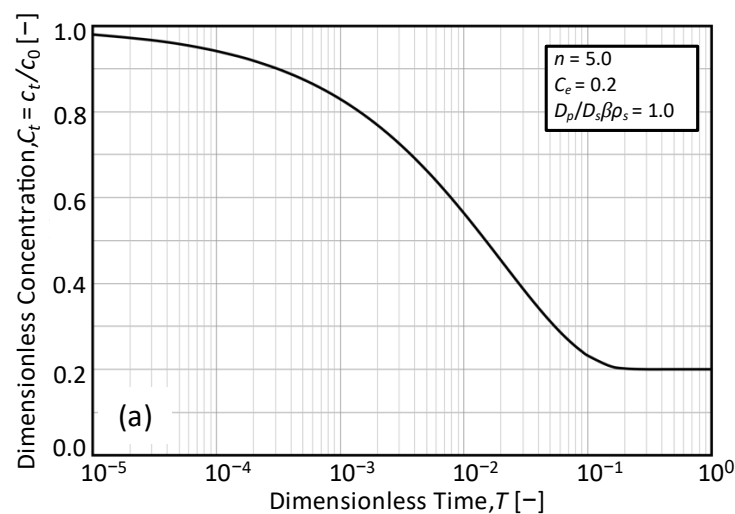


Figure 4. Cont.

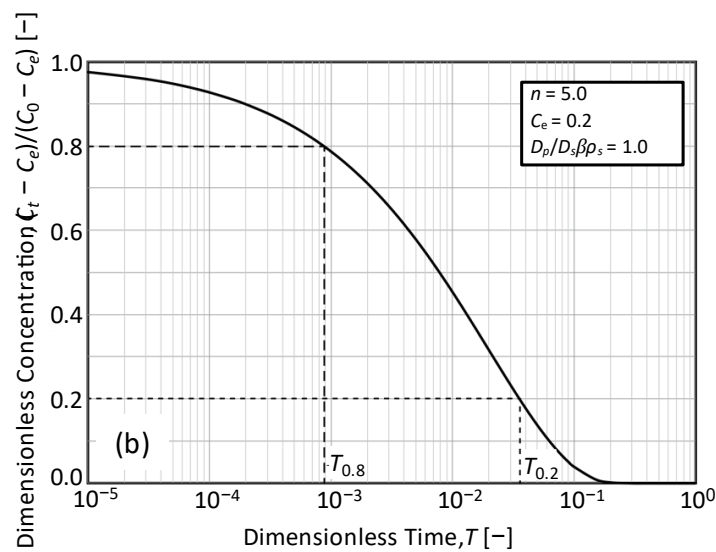


Figure 4. Typical numerical concentration decay curve. (a) Dimensionless concentration decay curve simulated based on parallel diffusion model, (b) reduced dimensionless concentration decay curve.

3.3. Relationship between $T_{0.2}/T_{0.8}$ and R_D

From the values of $T_{0.8}$ and $T_{0.2}$, which were used as an index of the concentration variation range of the NCDC, the $T_{0.2}/T_{0.8}$ value was determined. Thus, concentration decay curves were characterized using the dimensionless time ratio $T_{0.2}/T_{0.8}$. The NCDCs under various R_D values were calculated for the series of n and c_0 , and the relationship curve between $T_{0.2}/T_{0.8}$ and R_D values was obtained (Figure 5). The R_D value was obtained using the relationship shown in Figure 5 by comparing the numerical calculation results with the $T_{0.2}/T_{0.8}$ value determined experimentally by the CMBR method. This relationship also means that the value of $T_{0.2}/T_{0.8}$ depends on the diffusion coefficient in the phase with a larger adsorbate distribution. It can be seen from Figure 5 that the smaller the value of C_e , the more accurate the diffusion coefficient. For a more accurate determination of the pore and surface diffusivities, the $R_D = D_p/D_s\beta\rho_s$ values should be between 0.1 and 10. The procedure for using the experimental values is described as follows.

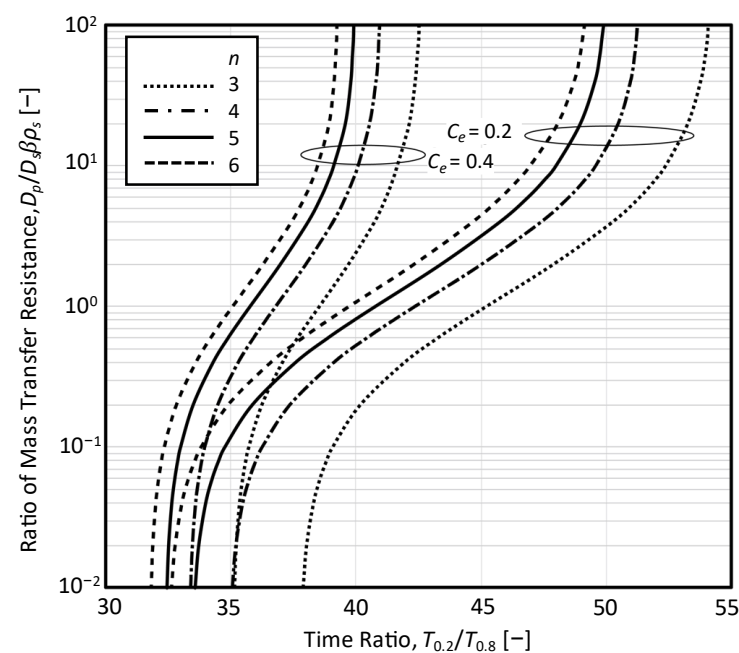


Figure 5. Dependency of mass transfer resistance ratio on the time ratio, $T_{0.2}/T_{0.8}$.

3.4. Determination Procedure with Experimental Data

Step 1. Determination of $T_{0.2}/T_{0.8}$

The experimental CMBR data obtained using *p*-nitrophenol as the adsorbate and granular activated carbon as the adsorbent were examined with a simple approach to determining the kinetic parameters in the parallel diffusion model from a single concentration decay curve. Experimental method details for the CMBR method are provided elsewhere [8]. Some details of the experimental conditions of the CMBR method are shown inside the squares in Figures 6 and 7. The concentration decay data of the adsorption system ($c_0 = 1447$ mg/L, $n = 6.2$, $V = 1$ L, $m = 1$ g, $m\beta/V = 1.0$) under negligible film mass transfer resistance conditions, which are reproducible and reliable from an experimental point of view, were used in this study. The experimentally obtained concentration decay curve is shown in Figure 6a, and the dimensional equilibrium concentration c_e was determined from the decay curve. The dimensionless equilibrium concentration in the CMBR vessel was obtained as $c_e/c_0 = 0.188$ for the system under study. Figure 6b shows a plot of $(C_t - C_e)/(C_0 - C_e)$ as the vertical axis. The values of $T_{0.8}$ and $T_{0.2}$ are given in Figure 6b, and it was found to be 41.1.

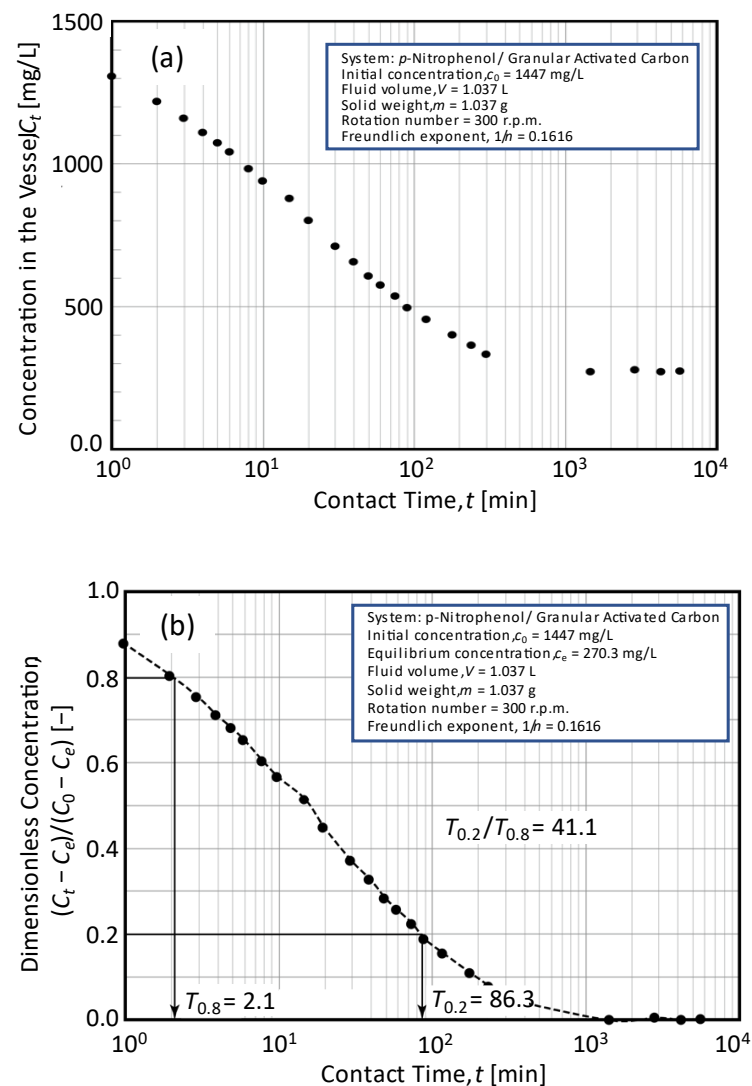


Figure 6. Experimental concentration decay curve. (a) Dimensional decay curve, (b) dimensionless decay curve.

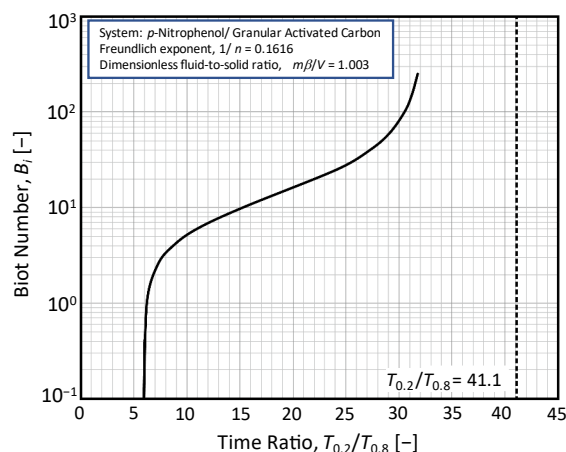


Figure 7. Determination of experimental Biot number.

Step 2. Confirmation of intraparticle diffusion-limited adsorption

The Freundlich exponent, $1/n$, and dimensionless fluid-to-solid ratio, $V/m\beta$, can be calculated from the experimental conditions and the relationship of the adsorption equilibrium. The concentration decay curves (NCDCs) in the CMBR were estimated by numerical calculations based on the model with fluid film and intraparticle diffusion transfer resistances. For obtaining a series of Biot numbers, the experimental values of $1/n$ and $V/m\beta$ were used. Figure 7 shows an illustration of the relationship between Biot numbers and $T_{0.2}/T_{0.8}$ values based on the NCDCs. The rate-limiting process in the system under consideration can be calculated from the $T_{0.2}/T_{0.8}$ value (=41.1) obtained from the experimental NCDC (dotted line in Figure 7). As seen in Figure 7, the mass transfer resistance in the fluid-to-solid film is negligible because of the very large Biot number condition of the adsorption experiment at $T_{0.2}/T_{0.8} = 41.1$. This step can be skipped when the film transfer is not obviously rate-limiting in the adsorption process. Nonetheless, this step is effective to ensure that the decay curve (adsorption data) is obtained under appropriate conditions for estimating the intraparticle diffusion coefficient, and the estimated diffusion coefficient is reliable.

Step 3. Determination of R_D

The NCDCs are calculated numerically using the experimentally obtained values of $1/n$ and $V/m\beta$ for a series of $R_D (=D_p/D_s\beta\rho_s)$ using the parallel diffusion model. The $T_{0.2}/T_{0.8}$ value was determined for each NCDC to obtain the relationship between R_D and $T_{0.2}/T_{0.8}$. The relationship between R_D and $T_{0.2}/T_{0.8}$ is shown in Figure 8, along with the $T_{0.2}/T_{0.8}$ value determined from the experiment. The value of R_D in the experimental system was found to be 1.75.

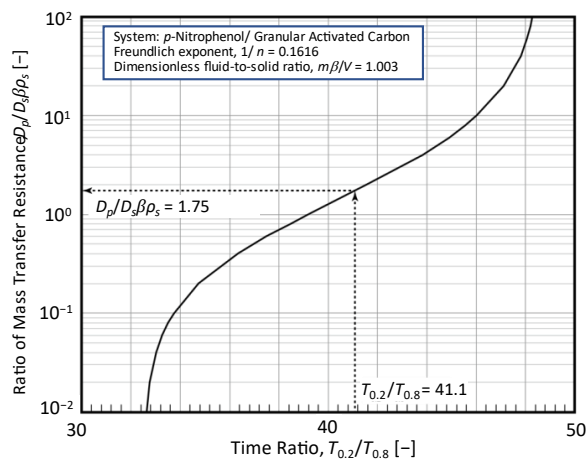


Figure 8. Relationship between R_D and $T_{0.2}/T_{0.8}$ values.

Step 4. Determination of D_s and D_p

The NCDC was recalculated using the parallel diffusion model with the known and determined parameters of $1/n = 0.1616$, $V/m\beta = 1.003$, and $R_D = D_p/D_s\beta\rho_s = 1.75$. The obtained NCDC values were compared with the experimental data, as shown in Figure 9. Then, the time ratio (T/t) of $3.9 \times 10^{-4} \text{ min}^{-1}$ was obtained (Figure 9). The value of D_s was estimated using Equation (14), based on the definition of the dimensionless variable T . Constant 60 is included in the equation for the conversion of time units from minutes to seconds.

$$D_s = 60 \left(\frac{T}{t} \right) r_p^2 = 60 \left(3.9 \times 10^{-4} \right) (0.03575)^2 = 8.31 \times 10^{-9} \text{ cm}^2/\text{s} \quad (14)$$

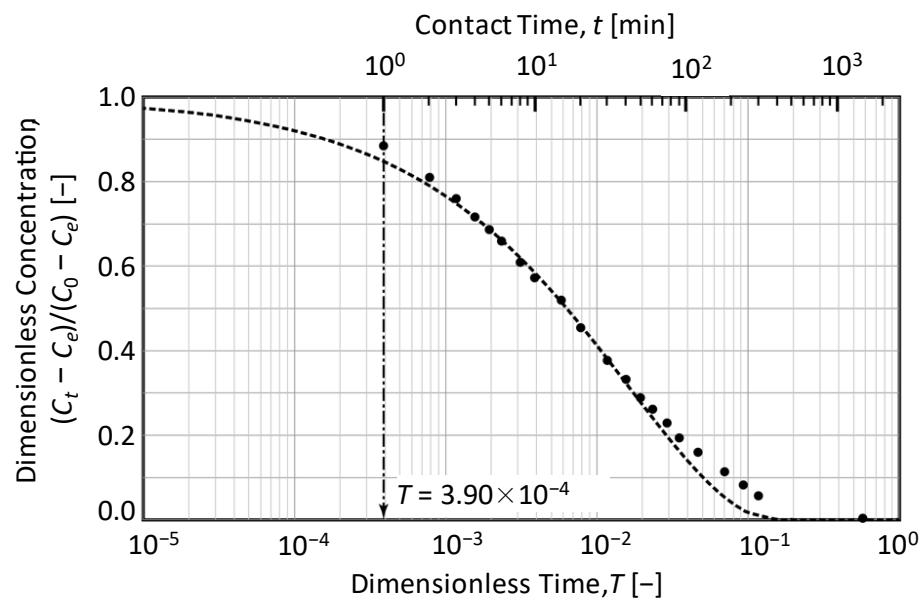


Figure 9. Comparison of the concentration decay curves obtained by the experiment and the numerical calculation of the theoretical model.

The value of D_p can be obtained from the R_D and D_s values, as shown in Equation (15).

$$D_p = R_D D_s \beta \rho_s = (3.9 \times 10^{-4}) (8.31 \times 10^{-9}) (0.3474) (484) = 1.40 \times 10^{-6} \text{ cm}^2/\text{s} \quad (15)$$

where $\beta = q_0/c_0 = kc_0^{1/n}/c_0$ [L/g], and ρ_s [g/L] denotes the apparent solid density.

The ratio of pore diffusivity (D_p) to molecular diffusivity (D_{AB}) is independent of the adsorption system and depends on the adsorbate used [1]. Wilke and Chan’s equation [31] was used to estimate the molecular diffusivity. For *p*-nitrophenol at 293.2 K, the value was 6.85×10^{-6} , and the value of D_p/D_{AB} was calculated to be 0.204. This value is similar to that of 0.22 reported by Furuya [8]. The efficiency of this method for determining the kinetic parameters in the parallel diffusion model was validated.

3.5. Summary of the Determination Procedure

The overall procedure for determining the kinetic parameters in the parallel diffusion model is shown in Figure 10. The graphs of R_D vs. $T_{0.2}/T_{0.8}$ and Biot number vs. $T_{0.2}/T_{0.8}$, as shown in Figures 5 and 7, respectively, can be prepared in advance for the conditions used in practice. The kinetic parameters examined in this study can be determined simply using graphs with a few batch adsorption experiments.

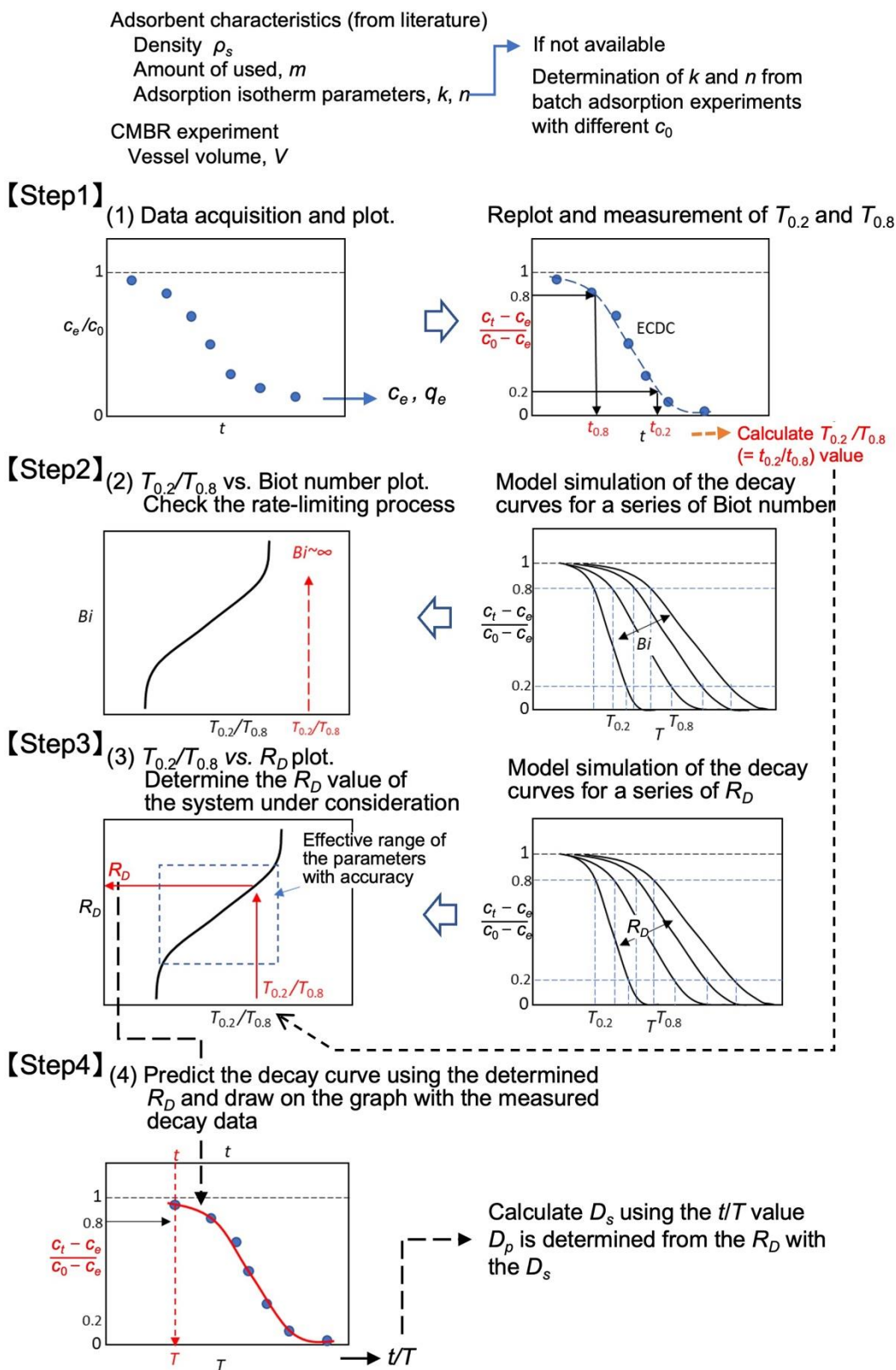


Figure 10. Determination procedure for the kinetic parameters.

4. Conclusions

In liquid-phase adsorption, the mass transfer within porous solids is dominated by pore and surface diffusion. Because these diffusions occur in parallel, the mechanism with low diffusion resistance is more dominant. In this study, the parallel diffusion model, a

simple method for obtaining pore and surface diffusivity from one experimental concentration decay curve, was examined using the CMBR technique. It was confirmed that both diffusion coefficients can be obtained from one concentration decay curve when the reactor's concentration change is sufficiently large and the fluid-to-solid mass transfer resistance is negligible.

Using the proposed method, real sample data were analyzed, and the validity of the calculated diffusivities was discussed. The ratio of pore diffusivity to effective molecular diffusivity was estimated using Chan's equation. The obtained value of 0.204 was comparable to the previously obtained results by other scholars.

Because the parallel diffusion model was used in this study, the diffusion mechanism with a smaller mass transfer resistance dominated the overall intraparticle diffusion. Therefore, the surface diffusion controlling model must be used when the R_D value is less than 0.1, and the pore diffusion controlling model should be applied when the R_D value is greater than 10.

Author Contributions: Conceptualization, E.F. and Y.S.; methodology, E.F. and Y.S.; software, E.F.; validation, Y.S., N.S. and K.E.N.; formal analysis, Y.S. and E.F.; investigation, Y.S. and E.F.; resources, E.F.; data curation, E.F. and Y.S.; writing—original draft preparation, Y.S.; writing—review and editing, Y.S.; visualization, E.F. and Y.S.; supervision, Y.S. and E.F.; project administration, E.F.; funding acquisition, E.F. All authors have read and agreed to the published version of the manuscript.

Funding: This work was supported by JSPS KAKENHI Grant Number 22K12416.

Data Availability Statement: Experimentally obtained data are presented in this study.

Conflicts of Interest: The authors declare no conflict of interest.

Nomenclature

| | | |
|-----------------|---|-------------------------------------|
| a_p : | Surface area based on solid particle | [cm ² /cm ³] |
| B_i : | Biot number = $k_f r_p / (D_s \beta \rho_s)$ | [-] |
| c_e : | Equilibrium concentration at time = infinity | [mg/L] |
| c_s : | Fluid concentration at $r = r_p$ | [mg/L] |
| c_t : | Concentration within the vessel at time t | [mg/L] |
| c_0 : | Concentration within the vessel at time = 0 | [mg/L] |
| C_m : | Dimensionless concentration | [-] |
| D_p : | Pore diffusivity | [cm ² /s] |
| D_s : | Surface diffusivity | [cm ² /s] |
| k_f : | Fluid film mass transfer coefficient | [cm/s] |
| m : | Weight of adsorbent | [g] |
| $1/n$: | Freundlich exponent | [-] |
| q_e : | Amount adsorbed in equilibrium with c_e | [mg/g] |
| q_t : | Average amount adsorbed within the adsorbent at time t | [mg/g] |
| q_0 : | Amount adsorbed at equilibrium with fluid concentration c_0 | [mg/g] |
| Q_m : | Dimensionless amount of adsorption | [-] |
| r : | Internal radial length (length from the solid center) | [cm] |
| r_p : | Particle radius | [cm] |
| R_D : | Ratio of diffusion resistance = $D_p / (D_s \beta \rho_s)$ | [-] |
| t : | Time | [min] |
| V : | Volume of the vessel | [L] |
| β : | q_0 / c_0 | [L/g] |
| ε : | Porosity | [-] |

References

1. Takeuchi, Y. *Chemical Engineers Handbook*, 5th ed.; Maruzen: Tokyo, Japan, 1988; pp. 595–598.
2. Bhatnagar, A.; Jain, A.K. A comparative adsorption study with different industrial wastes as adsorbents for the removal of cationic dyes from water. *J. Colloid Interf. Sci.* **2005**, *281*, 49–55. [[CrossRef](#)]

3. Ip, A.W.; Barford, J.P.; McKay, G. A comparative study on the kinetics and mechanisms of removal of reactive black 5 by adsorption onto activated carbons and bone char. *Chem. Eng. J.* **2010**, *157*, 434–442. [[CrossRef](#)]
4. Deryło-Marczewska, A.; Blachnio, M.; Marczewski, A.W.; Seczkowska, M.; Tarasiuk, B. Phenoxyacid pesticide adsorption on activated carbon—Equilibrium and kinetics. *Chemosphere* **2019**, *214*, 349–360. [[CrossRef](#)]
5. Bosacka, A.; Zienkiewicz-Strzałka, M.; Wasilewska, M.; Deryło-Marczewska, A.; Podkościelna, B. Physicochemical and adsorption characteristics of divinylbenzene-co-triethoxyvinylsilane microspheres as materials for the removal of organic compounds. *Molecules* **2021**, *26*, 2396. [[CrossRef](#)]
6. Wasilewska, M.; Marczewski, A.W.; Deryło-Marczewska, A.; Sternik, D. Nitrophenols removal from aqueous solutions by activated carbon—Temperature effect of adsorption kinetics and equilibrium. *J. Environ. Chem. Eng.* **2021**, *9*, 105459. [[CrossRef](#)]
7. Wasilewska, M.; Deryło-Marczewska, A. Adsorption of non-steroidal anti-inflammatory drugs on alginate-carbon composites—equilibrium and kinetics. *Materials* **2022**, *15*, 6049. [[CrossRef](#)]
8. Furuya, E.G.; Chang, H.T.; Miura, Y.; Yokomura, H.; Tajima, S.; Yamashita, S.; Noll, K.E. Intraparticle mass transport mechanism in activated carbon adsorption of phenols. *J. Environ. Eng.* **1996**, *122*, 909–916. [[CrossRef](#)]
9. Kannan, P.; Pal, P.; Banat, F. Design of adsorption column for reclamation of methyl-diethanolamine using homogeneous surface diffusion model. *Oil Gas Sci. Technol. Rev. IFP Energ. Nouv.* **2020**, *75*, 1–12. [[CrossRef](#)]
10. Eder, S.; Müller, K.; Azzari, P.; Arcifa, A.; Peydayesh, M.; Nyström, L. Mass transfer mechanism and equilibrium modelling of hydroxytyrosol Adsorption on Olive Pit-Derived Activated Carbon. *Chem. Eng. J.* **2021**, *404*, 126519. [[CrossRef](#)]
11. Kavand, M.; Fakoor, E.; Mahzoon, S.; Soleimani, M. An improved film-pore-surface diffusion model in the fixed-bed column adsorption for heavy metal ions: Single and multi-component systems. *Process Saf. Environ. Prot.* **2018**, *113*, 330–342. [[CrossRef](#)]
12. Ocampo-Pérez, R.; Leyva-Ramos, R.; Padilla-Ortega, E. Equilibrium and kinetic adsorption of organic compounds onto organo bentonite: Application of a surface diffusion model. *Adsorpt. Sci. Technol.* **2011**, *29*, 1007–1024. [[CrossRef](#)]
13. Medved', I.; Černý, R. Surface diffusion in porous media: A critical review. *Micropor. Mesopor. Mater.* **2011**, *142*, 405–422. [[CrossRef](#)]
14. Ma, Z.; Whitley, R.D.; Wang, N.-H.L. Pore and surface diffusion in multicomponent adsorption and liquid chromatography systems. *AIChE J.* **1996**, *42*, 1244–1262. [[CrossRef](#)]
15. Rosen, J.B. Kinetics of a fixed bed system for solid diffusion into spherical particles. *J. Chem. Phys.* **1952**, *20*, 387–394. [[CrossRef](#)]
16. Kavand, M.; Asasian, N.; Soleimani, M.; Kaghazchi, T.; Bardestani, R. Film-pore-[concentration-dependent] surface diffusion model for heavy metal ions adsorption: Single and multi-component systems. *Process Saf. Environ. Prot.* **2017**, *107*, 486–497. [[CrossRef](#)]
17. Ma, A.; Abushaikha, A.; Allen, S.J.; McKay, G. Ion exchange homogeneous surface diffusion modelling by binary site resin for the removal of nickel ions from wastewater in fixed beds. *Chem. Eng. J.* **2019**, *358*, 1–10. [[CrossRef](#)]
18. Souza, P.R.; Dotto, G.L.; Salau, N.P.G. Detailed numerical solution of pore volume and surface diffusion model in adsorption systems. *Chem. Eng. Res. Des.* **2017**, *122*, 298–307. [[CrossRef](#)]
19. Souza, P.R.; Dotto, G.L.; Salau, N.P.G. Statistical evaluation of pore volume and surface diffusion model in adsorption systems. *J. Environ. Chem. Eng.* **2017**, *5*, 5293–5297. [[CrossRef](#)]
20. Valderrama, C.; Gamisans, X.; de las Heras, X.; Farrán, A.; Cortina, J.L. Sorption kinetics of polycyclic aromatic hydrocarbons removal using granular activated carbon: Intraparticle diffusion coefficients. *J. Hazard. Mater.* **2008**, *157*, 386–396. [[CrossRef](#)]
21. Saripall, K.P.; Serne, R.J.; Meyer, P.D.; McGrail, B.P. Prediction of diffusion coefficients in porous media using tortuosity factors based on interfacial areas. *Ground Water.* **2002**, *40*, 346–352. [[CrossRef](#)]
22. Liu, B.J.; Yang, Y.W.; Ren, Q.L. Parallel pore and surface diffusion of levulinic acid in basic polymeric adsorbents. *J. Chromatogr. A* **2006**, *1132*, 190–200. [[CrossRef](#)] [[PubMed](#)]
23. Liu, B.; Zeng, L.; Mao, J.; Ren, Q. Simulation of levulinic acid adsorption in packed beds using parallel pore/surface diffusion model. *Chem. Eng. Technol.* **2010**, *33*, 1146–1152. [[CrossRef](#)]
24. Yao, C.; Chen, T. A new simplified method for estimating film mass transfer and surface diffusion coefficients from batch adsorption kinetic data. *Chem. Eng. J.* **2015**, *265*, 93–99. [[CrossRef](#)]
25. Chung, P.-L.; Bugayong, J.G.; Chin, C.Y.; Wang, N.H. A parallel pore and surface diffusion model for predicting the adsorption and elution profiles of lispro insulin and two impurities in gradient-elution reversed phase chromatography. *J. Chromatogr. A* **2010**, *1217*, 8103–8120. [[CrossRef](#)] [[PubMed](#)]
26. Brzić, D.V.; Petkovska, M.T. Nonlinear frequency response analysis as a tool for identification of adsorption kinetics: Case study—Pore-surface diffusion control. *Hindawi. Math. Probl. Eng.* **2019**, *2019*, 7932967. [[CrossRef](#)]
27. Petkovska, M.; Do, D.D. Nonlinear frequency response of adsorption systems. *Chem. Eng. Sci.* **1998**, *53*, 3081–3097. [[CrossRef](#)]
28. Costa, E.; Calleja, G.; Marijuan, L. Adsorption of Phenol and p-Nitrophenol on Activated Carbon: Determination of Effective Diffusion Coefficients. *Ads. Sci. Tech.* **1987**, *4*, 59–77. [[CrossRef](#)]
29. Shao, Y.; Chen, H. Adsorption kinetics of p-nitrophenol (PNP) on coal-based activated carbon: Experimental and simulation. *Desalin. Water Treat.* **2016**, *57*, 14496–14505. [[CrossRef](#)]
30. Fujiki, J.; Sonetaka, N.; Ko, K.-P.; Furuya, E. Experimental determination of intraparticle diffusivity and fluid film mass transfer coefficient using batch contactors. *Chem. Eng. J.* **2010**, *160*, 683–690. [[CrossRef](#)]
31. Wilke, C.R.; Chang, P. Correlation of diffusion coefficients in dilute solutions. *AIChE J.* **1955**, *1*, 264–270. [[CrossRef](#)]